International Journal for Innovative Engineering and Management Research
A Peer Revieved Open Access International Journal
www.ijiemr.org

# ASYMMETRICAL PWM FULL BRIDGE CONVERTER FED INDUCTION MOTOR DRIVE WITH RENEWABLE ENERGY SOURCE

P VARUN KUMAR
Assistant Professor, Department of Electrical and Electronics Engineering, Siddhartha Institute of Technology and Sciences, Narapally, Hyderabad, Telangana, India

**ABSTRACT-** : This paper proposes an improved topology asymmetrical full bridge DC-DC converter fed Induction motor has got the volatility of wide range of speed control. Power electronic converters can envisage dynamic speed control. The front end rectifier and dc to dc converter can be monitored to facilitate requisite Input voltage to the inverter fed drive working at constant speed. Renewable energy source is utilized, extended voltage and power output, less maintenance and higher fault tolerance, the asymmetrical PWM full bridge converter are good, for utility interface of various renewable energy sources. Consequently, the energy in the leakage inductance is transferred to the load without causing reverse recovery losses in the output diodes. This allows higher switching frequencies and, therefore, an increase in power density. This dissertation proposes a new PWM converter topology and control scheme. Optimal component values are calculated to minimize losses in the complete operating range and to assess which measure is best suited. The topologic is full bridge asymmetrical DC-DC converter and Induction Motor drive system. The simulation results are presented by using Matlab/Simulink software.

**Index Terms**—Asymmetrical pulse-width modulated (PWM), full-bridge converter, soft switching, Induction Motor, PV System.

## I. INTRODUCTION

Solar energy is the most low cost, competition free, universal source of energy as sun shines throughout. This energy can be converted into useful electrical energy using photovoltaic technology. The steady state reduction of price per peak watt and simplicity with which the installed power can be increased by adding panels are attractive features of PV technology. Among the many applications of PV energy, pumping [1-2] is the most promising. In a PV pump storage system, solar energy is stored, when sunlight is available as potential energy in water reservoir and consumed according to demand. There are advantages in avoiding the use of large banks of lead acid batteries, which are heavy and expensive and have one fifth of the lifetime of a PV panel. A number of simulation DC motor driven PV pumps are already in use in several parts of the world, but they suffer from maintenance problems due to the presence of the commutator and brushes. Hence a pumping system based on an induction motor can be an attractive proposal where reliability and maintenance-free operations with

less cost are important. The effective operation of Induction motor is based on the choice of

International Journal for Innovative Engineering and Management Research
A Peer Revieved Open Access International Journal
www.ijiemr.org

suitable converter-inverter system that is fed to Induction Motor. For PV applications like pumping these converters could do a good job as pumping is carried out at high power. Thus a new push pull converter which is two switch topology can do justice by giving a high power throughout [3-4]. The Induction Motors are the AC motors and hence from converter, an inverter system is also required to obtain an AC voltage. This inverter is chosen based on its advantages [5] and it is fed to induction motor. Photovoltaic technology is one of the most promising for distributed low-power electrical generation. The steady reduction of price per peak watt over recent years and the simplicity with which the installed power can be increased by adding panels are some of its attractive features [6-7]. Among the many applications of photovoltaic energy, pumping is one of the most promising. In a photovoltaic pump-storage system, solar energy is stored, when sunlight is available, as potential energy in a water reservoir and then consumed according to demand. Most of the industrial drives use ac induction motor because these motors are rugged, [8-10] reliable, and relatively inexpensive. Induction motors are mainly used for constant speed applications because of unavailability of the variable frequency supply voltage but many applications [11-12] need variable speed operations. Historically, mechanical gear systems were used to obtain variable speed. Recently, power electronics and control systems have matured to allow these components to be used for motor control in place of mechanical gears. Present day drive types are the Induction motor

drives with voltage source inverters. Also the voltage waveforms of traditional two level inverter fed Induction motor shows that the voltage across the motor contains not only the required "fundamental" sinusoidal components, but also pulses of voltage i.e. "ripple "voltage [13]. The recent advancement in power electronics has initiated to improve the level of inverter instead increasing the size of filter. The total harmonic distortion of the classical inverter is very high [14]. The performance of the multilevel inverter is better than classical inverter. In other words the total harmonic distortion for multilevel inverter is low. The total harmonic distortion is analyzed between multilevel inverter and other classical inverter. To get the speed control of induction motor, we need vary both voltage and current. This technique is called as constant V/F [15] method. By choosing the suitable inverter we can vary both voltage and frequency of the induction motor to get the required speed control.

## II ANALYSIS OF A PWM FULL-BRIDGE CONVERTER

### A. Circuit Configuration and Operation Principle

A circuit configuration of the highly efficient APWM full bridge converter for low input voltage range is shown in Fig.2. The configuration of the proposed converter is basically similar to that of the conventional full-bridge converter except for the dc blocking capacitor and the secondary side of the transformer. The primary side of the transformer consists of the primary winding turns $N_p$, the four switches, and the dc blocking capacitor $C_b$. The secondary side has the secondary winding $N_s$, the output diode $D_o$, and the output capacitor $C_o$.

International Journal for Innovative Engineering and Management Research
A Peer Revieved Open Access International Journal
www.ijiemr.org

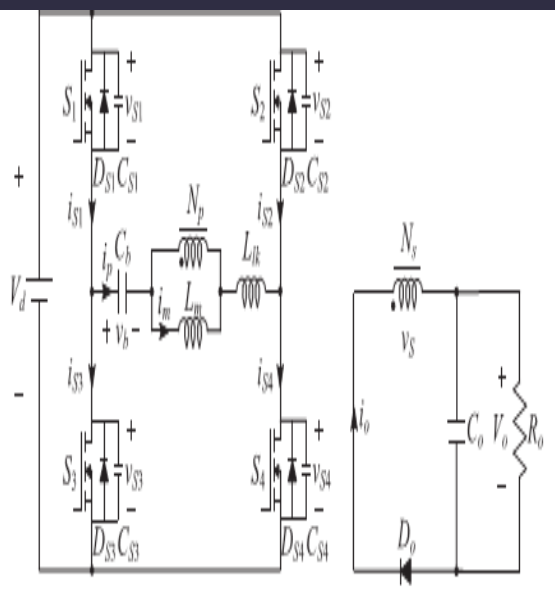

Fig.2.Circuit diagram of the proposed APWM full-bridge converter

To analyze the steady-state operation of the proposed APWM full-bridge converter, the following assumptions are made.

1) The transformer is modeled as an ideal transformer with the primary winding turns $N_p$, the secondary winding turns $N_s$, the magnetizing inductance $L_m$, and the leakage inductance $L_{lk}$
2) All switches $S_1$–$S_4$ are considered as ideal switches except for their body diodes and output capacitors ($C_{S1}$=$C_{S2}$=$C_{S3}$=$C_{S4}$= $C_{oss}$).
3) The dc blocking capacitor $C_b$ and the output capacitor $C_o$ are large enough to neglect the voltage ripple on it, so the voltages across $C_b$ and $C_o$ are constant.

While the switch $S_1$ ($S_4$) operates with a duty ratio D, depending on the input voltage and load condition, the switch $S_2$ ($S_3$) operates with a duty ratio 1−D. In other words, the switches $S_1$ ($S_4$) and $S_2$ ($S_3$) are operated asymmetrically. Therefore, the circulating current loss of the primary side can be eliminated because the proposed converter has no freewheeling period.

Fig. 3 represents the operating modes, and Fig.4 represents the theoretical waveforms of the proposed converter under a steady-state condition. The operation of the proposed converter can be divided into six modes during a switching period $T_s$.

**Mode 1** ***[$t_0$, $t_1$]:*** At $t_0$, the switches $S_2$ and $S_3$ are turned off. The primary current $i_p$ discharges the output capacitances $C_{S1}$ and $C_{S4}$ of the switches $S_1$ and $S_4$ and charges the output capacitances $C_{S2}$ and $C_{S3}$ of switches $S_2$ and $S_3$. The interval of this mode is very short and negligible because the output capacitances $C_{oss}$ of the switches are very small. Thus, the primary current $i_p$ and the magnetizing current $i_m$ are regarded as constant value.

**Mode 2** ***[$t_1$, $t_2$]:*** At $t_1$, when the voltages $v_{S1}$ and $v_{S4}$ across the switches $S_1$ and $S_4$ become zero, the negative current flows through their body diodes $D_{S1}$ and $D_{S4}$before the switches $S_1$ and $S_4$ are turned on. Then, ZVS operation is achieved with the turn-on of the switches $S_1$ and $S_4$, and the resonance occurs between the dc blocking capacitor $C_b$ and the primary inductor $L_m$ + $L_{lk}$ of the transformer, but resonance effect does not appear because the resonant period is much longer than one switching period $T_s$. Thus, by the difference between the voltages of the input and the dc blocking capacitor $C_b$, the direction of the primary current $i_p$ is changed and kept almost linearly as follows:

$$i_p(t) = i_p(t_1) + \frac{V_d - V_b}{L_m + L_{lk}}(t - t_1) \quad (1)$$

Where $V_d$ is the input voltage and $V_b$ is the average voltage across the dc blocking capacitor $C_b$.

International Journal for Innovative Engineering and Management Research
A Peer Revieved Open Access International Journal
www.ijiemr.org

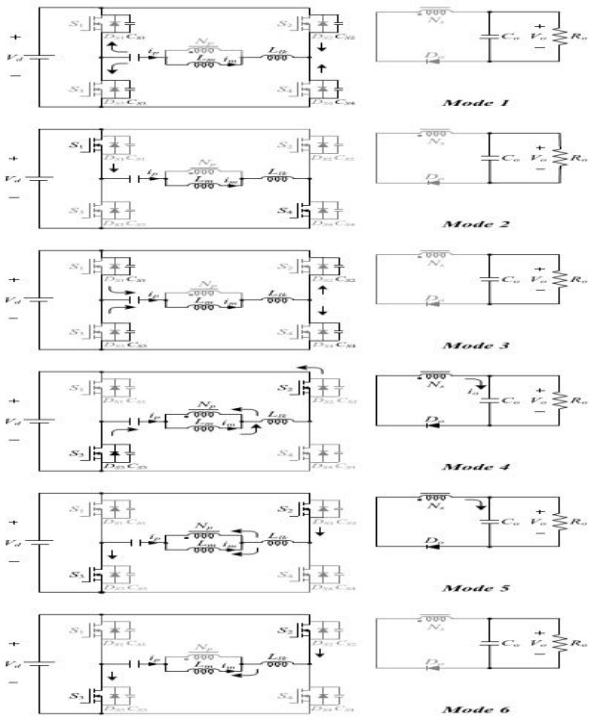


Fig.3. Operating modes of the proposed converter

**Mode 3 [$t_2$, $t_3$]:** At $t_2$, the switches $S_1$and $S_4$ are turned off. The primary current ip charges the output capacitances $C_{S1}$, $C_{S4}$ of $S_1$, $S_4$ and discharges the output capacitances $C_{S2}$, $C_{S3}$ of $S_2$, $S_4$. Similar to Mode 1, the primary current $i_p$ and the magnetizing current $i_m$ are regarded as constant value.

**Mode 4 [$t_3$, $t_4$]:** At $t_3$, similar to Mode 2, ZVS turn-on of the switches $S_2$ and $S_3$ is achieved. The energy stored in the magnetizing inductance is delivered to the secondary side of transformer, and the voltage across the magnetizing inductance $L_m$ is clamped by the reflected output voltage as

$$L_m \frac{di_m(t)}{dt} = -\frac{V_o}{n} \tag{2}$$

Where $n=N_s/N_p$. Because the difference between the primary current $i_p$ and the magnetizing current $i_m$ is reflected in the output current $i_o$, the magnetizing current $i_m$ is decreased as

$$i_m(t) = i_p(t_3) - \frac{V_o}{nL_m}(t - t_3) \tag{3}$$

The resonance occurs between the dc blocking capacitor $C_b$ and the leakage inductance $L_{lk}$ of the transformer. The voltage across the leakage inductance $L_{lk}$ of primary side is the difference between $V_d + V_b$ and the reflected output voltage $V_o/n$ from the secondary side. Thus, the state equations can be written as follows:

$$L_{lk} \frac{di_p(t)}{dt} = -V_d - V_b + \frac{V_o}{n} \tag{4}$$

$$C_b \frac{dv_b(t)}{dt} = i_p(t) \tag{5}$$

Solving (4) and (5), the primary current $i_p$ is

$$i_p(t) = i_p(t_3)\cos\omega_r(t - t_3) + \frac{V_o/n - V_d - V_b}{Z_r}\sin\omega_r(t - t_3) \tag{6}$$

Where the resonant angular frequency $\omega_r$ and the impedance $Z_r$ of the resonant circuit are

$$Z_r = \sqrt{\frac{L_{lk}}{C_b}} \quad \omega_r = \frac{1}{\sqrt{L_{lk}C_b}} \tag{7}$$

**Mode 5 [$t_4$, $t_5$]:** At $t_4$, the primary current $i_p$ becomes zero and changes its direction. Also, the magnetizing current im changes its direction during this interval. The output current $i_o$ approaches zero at the end of this mode with resonant characteristics. When the output current $i_o$ becomes zero, this mode ends.

**Mode 6 [$t_5$, $t_6$]:** At $t_5$, because the resonance launched in Mode 4 is ended, the output current $i_o$ becomes zero. However, the output diode $D_o$ is maintained to on-state until the switches $S_2$ and $S_3$ are turned off. During this mode, the primary current $i_p$ is equal to the magnetizing current $i_m$. Thus, ZCS turn-off of the output diode $D_o$ is achieved.

International Journal for Innovative Engineering and Management Research
A Peer Revieved Open Access International Journal
www.ijiemr.org

### B. Steady-State Analysis

While the switches $S_1$ and $S_4$ operate with a duty ratio $D$, the difference between the input voltage $V_d$ and the average voltage $V_b$ of the dc blocking capacitor $C_b$ is applied on the inductor of the transformer primary side. While the switches $S_2$ and $S_3$ operate with a duty ratio $1-D$, the reflected output voltage $V_o/n$ is applied on the inductor of the transformer primary side and the output diode $D_o$ is turned-on. Since the resonant period of the resonant network is much longer than the dead-time duration, equations of the primary current $i_p$ from (1) and (2) are derived as follows:

$$i_p(t_3) = i_p(t_1) + \frac{V_d - V_b}{L_m + L_{lk}} DT_s \tag{8}$$

$$i_p(t_1) = i_p(t_3) - \frac{V_o}{nL_m}(1-D)T_s \tag{9}$$

From the resonance of the primary side in Modes 4 and 5, since the leakage inductance $L_{lk}$ is much smaller than the magnetizing inductance $L_m$, the leakage inductance $L_{lk}$ is negligible. Therefore, the following equation can be obtained:

$$V_d + V_b \simeq \frac{V_o}{n} \tag{10}$$

From (8) to (10), the voltage gain between the input voltage $V_d$ and output voltage $V_o$ is expressed as follows:

$$\frac{V_o}{V_d} \simeq \frac{L_m}{L_m + L_{lk}} 2nD \simeq 2nD \tag{11}$$

Because the leakage inductance $L_{lk}$ is negligible, the average voltage $V_b$ of the dc blocking capacitor $C_b$ is expressed from (10) and (11) as shown in

$$V_b = V_d(2D-1) \tag{12}$$

Due to the charge balance of the dc blocking capacitor $C_b$, the average value of the primary current $I_p$ is zero in the steady state. Thus, the relation between the average values of the magnetizing current $I_m$and average output current $I_o$ can be determined as follows:

$$I_m - I_p = I_m - \frac{1}{T_s}\int_0^{T_s} i_p(t)dt = nI_o. \tag{13}$$

From Fig.4, the average magnetizing current $I_m$ can also be obtained by

$$I_m = \frac{i_p(t_1) + i_p(t_3)}{2}. \tag{14}$$

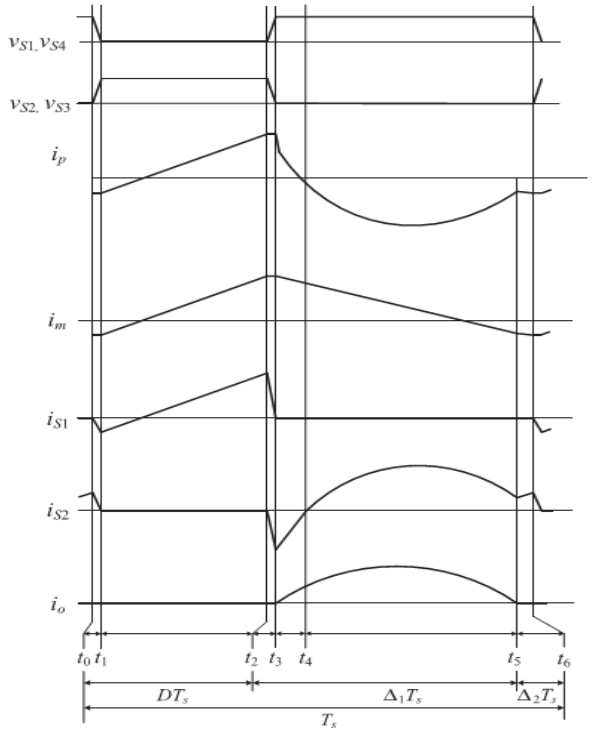


Fig.4.Theoretical waveforms of the proposed converter

From (1), (13), and (14), the currents $i_p$ ($t_1$) and ip ($t_3$) are given by

$$i_p(t_1) = nI_o - \frac{(1-D)T_s}{nL_m} V_o \tag{15}$$

International Journal for Innovative Engineering and Management Research
A Peer Revieved Open Access International Journal
www.ijiemr.org

$$i_p(t_3) = nI_o + \frac{(1-D)T_s}{nL_m}V_o \tag{16}$$

Using (13)–(16), the resonant current (6) can be represented by

$$i_p(t) = \left(nI_o + \frac{(1-D)T_s}{nL_m}V_o\right)\cos\omega_r(t-t_3) - \frac{V_o}{nL_m\omega_r}\sin\omega_r(t-t_3). \tag{17}$$

## III. SOFT-SWITCHING CONDITIONS

### A. ZVS Condition of the Power Switches

For ZVS turn-on of $S_1$ and $S_4$, the primary current $i_p$ ($t_1$) should be negative before $S_1$ and $S_4$ are turned on. Thus, from (15), ZVS condition can be expressed as follows:

$$nI_o - \frac{(1-D)T_s}{nL_m}V_o < 0. \tag{18}$$

Equation (18) is arranged by the min–max theorem as

$$\frac{n^2L_mI_{o,\max}}{V_o} = \frac{n^2L_m}{R_{o,\min}} < (1-D_{\max})T_s \tag{19}$$

Where $I_{o,max}$ is the maximum output current, $R_{o,min} = V_o/I_{o,max}$ is the minimum output resistance, and $D_{max}$ is the maximum duty ratio of the switches $S_1$ and $S_4$under the minimum input voltage $V_{d,min}$. From (3.11), $D_{max}$ can be described as

$$D_{\max} \simeq \frac{V_o}{2nV_{d,\min}}. \tag{20}$$

According to the variations of the input voltage $V_d$ and turn ratio, the duty ratio of the switches $S_1$ and $S_4$. Thus, from (19) and (20), the magnetizing inductance $L_m$ should be designed to satisfy ZVS condition as follows:

$$L_m < \left(1 - \frac{V_o}{2nV_{d,\min}}\right)T_s \cdot \frac{R_{o,\min}}{n^2} \tag{21}$$

Where $T_s$ is a switching period. According to the variation of the duty ratio $D$, the critical magnetizing inductance value $L_m$ to satisfy the ZVS turn-on condition of the switches The ZVS turn-on condition of the switches $S_2$ and $S_3$ can be expressed with the same manner of ZVS condition of the switches $S_1$and $S_4$. Thus, ZVS operation of $S_2$ and $S_3$ can be achieved when the primary current $i_p$ ($t_3$) is positive. From (16), ZVS condition of $S_2$ and $S_3$ is expressed as follows:

$$nI_o + \frac{(1-D)T_s}{nL_m}V_o > 0. \tag{22}$$

The left side terms of (22) are always positive regardless of load variations. Therefore, ZVS operation of the switches $S_2$ and $S_3$ can always is satisfied.

Another ZVS turn-on operation requires a sufficient dead time between two switch pairs to absolutely discharge the voltage across the output capacitance $C_{oss}$ of the switches. Because $i_p$ ($t_1$) = $i_m$ ($t_1$) is regarded as constant value during the dead time, the minimum dead time $\Delta t_{dead}$ can be calculated as

$$\min\{|i_p(t_1)|, |i_p(t_3)|\} \geq 4C_{oss}\frac{dV_d}{dt} \tag{23}$$

From (15) and (16), the primary current $i_p$ ($t_3$) is always larger than the absolute value of the primary current $i_p$ ($t_1$). Therefore, (23) can be simplified as

$$\Delta t_{dead} \geq \frac{C_{oss}V_d}{|i_p(t_1)|/4}. \tag{24}$$

The primary current $i_p$ ($t_1$) should be negative for ZVS operation. Thus, (24) can be expressed as shown in

International Journal for Innovative Engineering and Management Research
A Peer Revieved Open Access International Journal
www.ijiemr.org

$$\Delta t_{dead} \geq \frac{4C_{oss}V_d}{\frac{(1-D)T_s}{nL_m}V_o - nI_o} \quad (25)$$

The minimum dead time $\Delta t_{dead}$ should be considered in the practical design of the magnetizing inductance because $\Delta t_{dead}$ is always smaller than $(1-D_{max})\,T_s$.

### B. ZCS Condition of the Output Diode

To achieve the ZCS turn-off condition of the output diode $D_o$, the resonant angular frequency ωr should be larger than the critical angular frequency $\omega_{rc}$. Because the critical condition is ip (Ts) = $i_m(T_s)$ at $\Delta_2 T_s = 0$ and $D = D_{max}$, the critical angular frequency $\omega_{rc}$ can be described considering the negligible dead-time duration of the power switches as follows:

$$\left(\frac{n^2L_m}{R_{o,\min}} + t_{S2,\min}\right)\cos\omega_{rc}t_{S2,\min} - \frac{1}{\omega_{rc}}\sin\omega_{rc}t_{S2,\min} - \frac{n^2L_m}{R_{o,\min}} + t_{S2,\min} = 0 \quad (26)$$

Where $t_{S2,min}$ is the minimum turn-on duration of the switches $S_2$ and $S_3$. The magnetizing inductance $L_m$ is generally designed for the magnetizing current $i_m$ ($t_1$) to be a small negative value to minimize the conduction loss of the converter. By this assumption, (26) can be obtained as follows:

$$\tan\omega_{rc}t_{S2,\min} \simeq \omega_{rc}\frac{n^2L_m}{R_{o,\min}} + \omega_{rc}t_{S2,\min} \quad (27)$$

From (21), (27) is expressed as shown in

$$\tan\omega_{rc}t_{S2,\min} < 2\omega_{rc}t_{S2,\min} \quad (28)$$

Thus, the critical angular frequency $\omega_{rc}$ can be calculated using a numerical method as shown in

$$\omega_{rc} \approx \frac{\pi + 1.462}{t_{S2,\min}} = \frac{\pi + 1.462}{(1 - D_{\max})T_s} \quad (29)$$

From (29), the dc blocking capacitance $C_b$ must satisfy the following relation:

$$C_b \leq \frac{1}{\omega^2{}_{rc}L_{lk}} \quad (30)$$

According to the variation of the duty ratio $D$, the critical resonant capacitance $C_b$ to satisfy the ZCS turn-off condition of the output diode $D_o$.

## IV. INDUCTION MOTOR

An asynchronous motor type of an induction motor is an AC electric motor in which the electric current in the rotor needed to produce torque is obtained by electromagnetic induction from the magnetic field of the stator winding. An induction motor can therefore be made without electrical connections to the rotor as are found in universal, DC and synchronous motors. An asynchronous motor's rotor can be either wound type or squirrel-cage type.Three-phase squirrel-cage asynchronous motors are widely used in industrial drives because they are rugged, reliable and economical. Single-phase induction motors are used extensively for smaller loads, such as household appliances like fans. Although traditionally used in fixed-speed service, induction motors are increasingly being used with variable-frequency drives (VFDs) in variable-speed service. VFDs offer especially important energy savings opportunities for existing and prospective induction motors in variable-torque centrifugal fan, pump and compressor load applications. Squirrel cage induction motors are very widely used in both fixed-speed and variable-frequency drive (VFD)

applications. Variable voltage and variable frequency drives are also used in variable-speed service.In both induction and synchronous motors, the AC power supplied to the motor's stator creates a magnetic field that rotates in time with the AC oscillations. Whereas a synchronous motor's rotor turns at the same rate as the stator field, an induction motor's rotor rotates at a slower speed than the stator field. The induction motor stator's magnetic field is therefore changing or rotating relative to the rotor. This induces an opposing current in the induction motor's rotor, in effect the motor's secondary winding, when the latter is short-circuited or closed through external impedance. The rotating magnetic flux induces currents in the windings of the rotor; in a manner similar to currents induced in a transformer's secondary winding(s). The currents in the rotor windings in turn create magnetic fields in the rotor that react against the stator field. Due to Lenz's Law, the direction of the magnetic field created will be such as to oppose the change in current through the rotor windings. The cause of induced current in the rotor windings is the rotating stator magnetic field, so to oppose the change in rotor-winding currents the rotor will start to rotate in the direction of the rotating stator magnetic field. The rotor accelerates until the magnitude of induced rotor current and torque balances the applied load. Since rotation at synchronous speed would result in no induced rotor current, an induction motor always operates slower than synchronous speed. The difference, or "slip," between actual and synchronous speed varies from about 0.5 to 5.0% for standard Design B torque curve induction motors. The induction machine's essential character is that it is created solely by induction instead of being separately excited as in synchronous or DC machines or being self-magnetized as in permanent magnet motors.For rotor currents to be induced the speed of the physical rotor must be lower than that of the stator's rotating magnetic field ($n_s$); otherwise the magnetic field would not be moving relative to the rotor conductors and no currents would be induced. As the speed of the rotor drops below synchronous speed, the rotation rate of the magnetic field in the rotor increases, inducing more current in the windings and creating more torque. The ratio between the rotation rate of the magnetic field induced in the rotor and the rotation rate of the stator's rotating field is called slip. Under load, the speed drops and the slip increases enough to create sufficient torque to turn the load. For this reason, induction motors are sometimes referred to as asynchronous motors. An induction motor can be used as an induction generator, or it can be unrolled to form a linear induction motor which can directly generate linear motion.

**Synchronous Speed:**

The rotational speed of the rotating magnetic field is called as synchronous speed.

$$Ns = \frac{120 \times f}{P} \quad (RPM) \tag{31}$$

Where, f = frequency of the supply

P = number of poles

**Slip:**

Rotor tries to catch up the synchronous speed of the stator field, and hence it rotates. But in practice, rotor never succeeds in catching up. If rotor catches up the stator speed, there won't be any relative speed between the stator flux and the rotor, hence no induced rotor current and no torque production to maintain the rotation. However, this won't stop the motor, the rotor will slow down due to lost of torque, and the

International Journal for Innovative Engineering and Management Research
A Peer Revieved Open Access International Journal
www.ijiemr.org

torque will again be exerted due to relative speed. That is why the rotor rotates at speed which is always less the synchronous speed.

The difference between the synchronous speed (Ns) and actual speed (N) of the rotor is called as slip.

$$\% \text{ slip } \quad s = \frac{Ns - N}{Ns} \times 100 \qquad (32)$$

## V. MATLAB/SIMULATION RESULTS

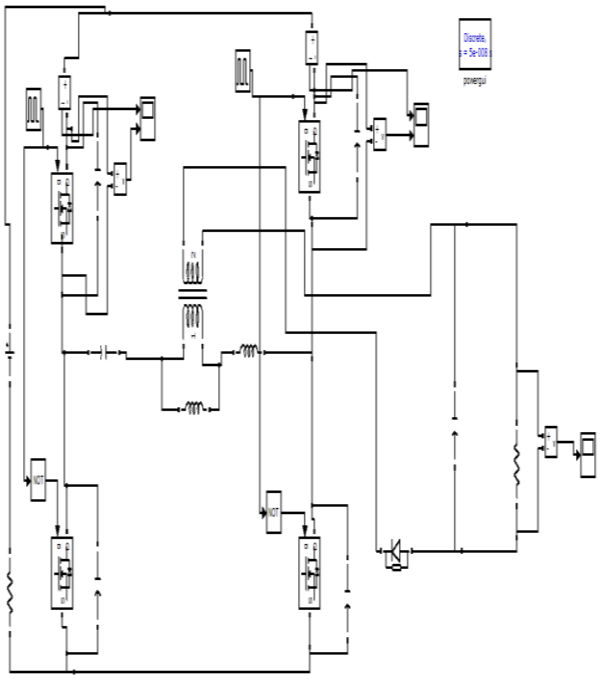

Fig.5.Matlab/Simulation model of proposed APWM Full Bridge Converter

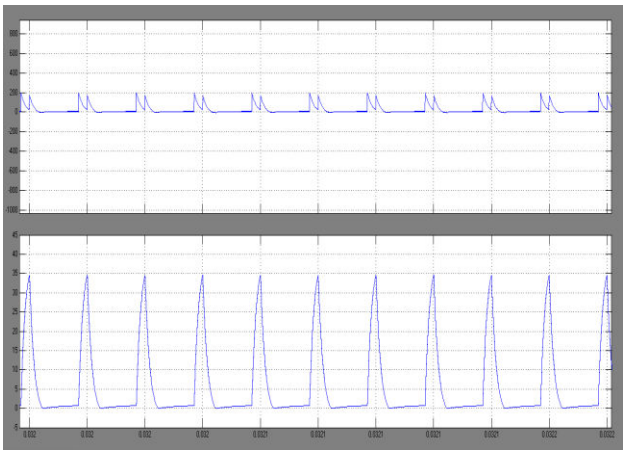

(a)

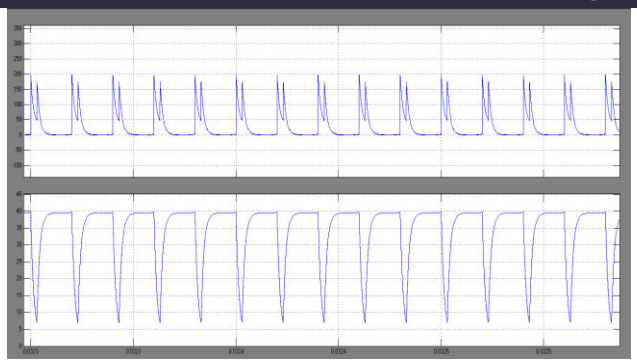

(b)

Fig.6. Simulation waveforms for ZVS turn-on of the switches S1 and S2 at Vd = 40 V and Po = 400 W. (a) vS1 and iS1. (b) vS2 and iS2.

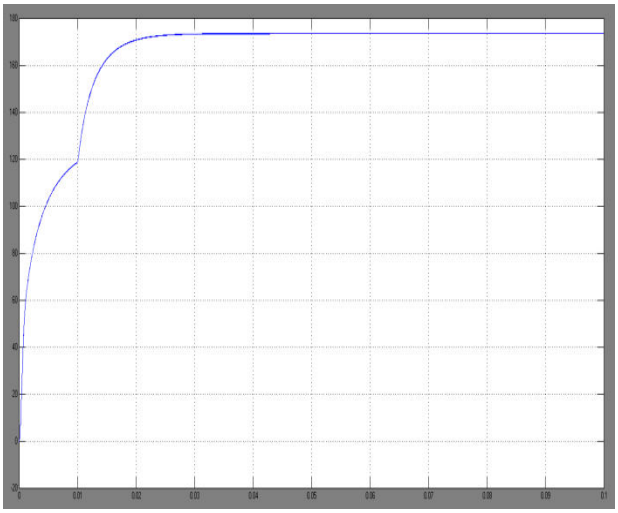

Fig.7.Simulation results for proposed converter output Voltage.

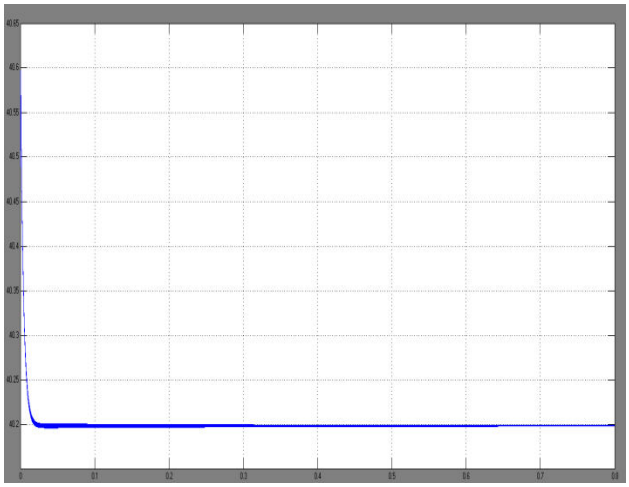

Fig.8 Simulation waveform of PV output voltage

International Journal for Innovative Engineering and Management Research
A Peer Revieved Open Access International Journal
www.ijiemr.org

(a)

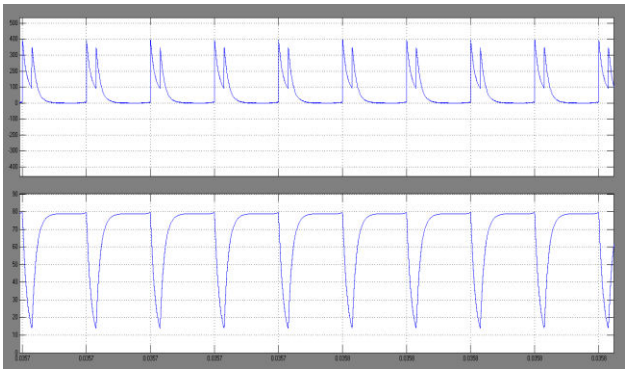

(b)

Fig.9. Simulation waveforms for ZVS turn-on of the switches S1 and S2 at Vd = 80 V and Po = 400 W. (a) vS1 and iS1. (b) vS2 and iS2.

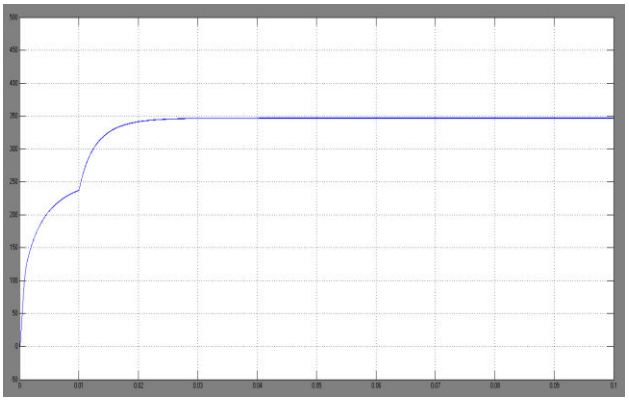

Fig.10.Simulation results for proposed converter output Voltage.

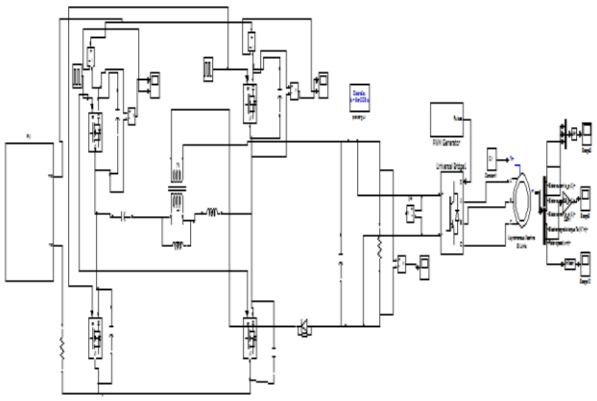

Fig.11.Matlab/Simulation model of PV with proposed APWM Full Bridge Converter fed induction motor drive

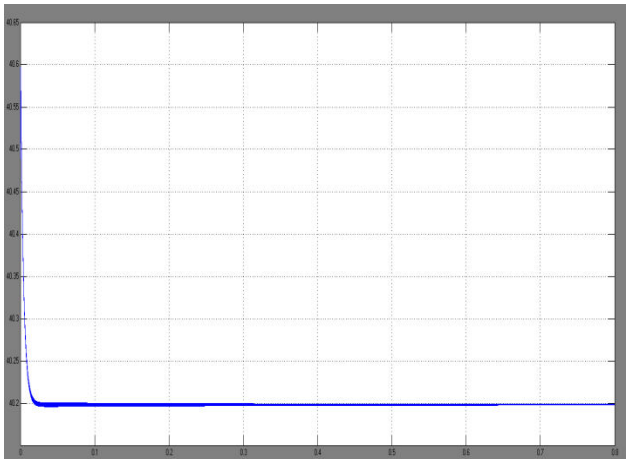

Fig.12 Simulation waveform of PV output voltage

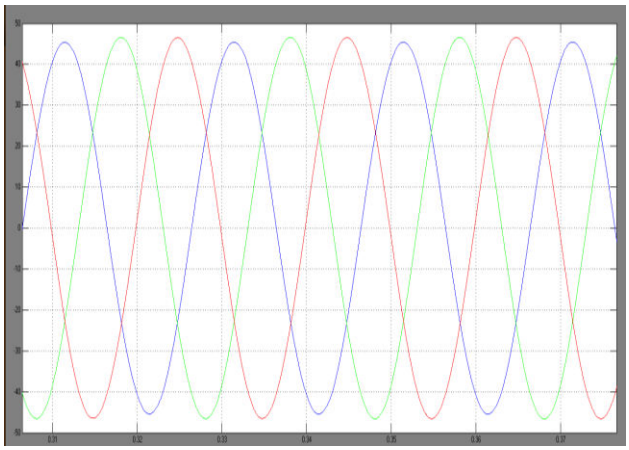

Fig.13.Simulation waveform of induction motor current

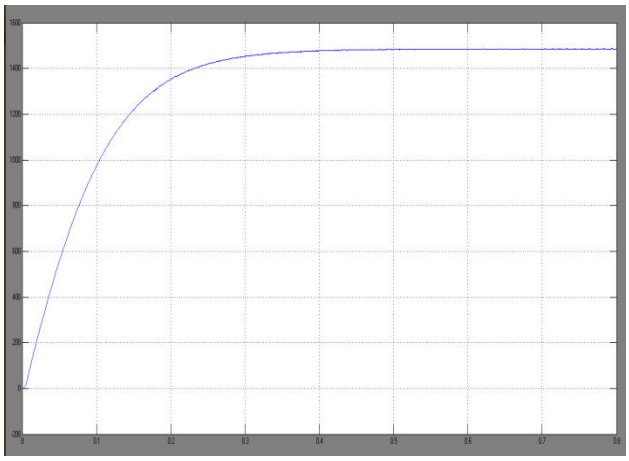

Fig.14 Simulation waveform of induction motor speed

International Journal for Innovative Engineering and Management Research
A Peer Revieved Open Access International Journal
www.ijiemr.org

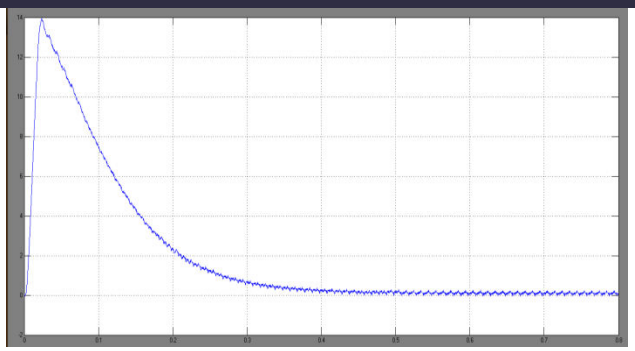

Fig.15 Simulation waveform of induction motor torque

## VI. CONCLUSION

Renewable system using asymmetrical full bridge converter with induction motor controlling is designed and analyzed. The Induction Motor can be effectively driven by single photovoltaic panel. Pulse Width Modulation Techniques usually increases the output voltage of the inverter and decreases the ripples. Finally the system performance is increased by the application of PWM Technique. All power switches operate under ZVS and output diode operates under ZCS without extra components. Also, all power switches are clamped to the input voltage. Thus, the proposed converter has the structure to minimize power losses. These advantages make the proposed converter suitable for fluctuating input voltage on renewable energy conversion systems. Matlab based model is developed and simulation results are showed for Isolated DC-DC converter fed induction motor. The proposed drive has demonstrated good speed control with energy efficient operation .The drive system is used for ac compressor unit in the wide range of speed and input AC voltage. The additional advantage of the present proposed application eliminates the AC unit switching and further consequent disturbances in the distribution system.

## REFERENCES

[1] J. Zhang, H. Wu, X. Qin, and Y. Xing, "PWM plus secondary-side phase-shift controlled soft-switching full-bridge three-port converter for renewable power systems," IEEE Trans. Ind. Electron., vol. 62, no. 11, pp. 7061–7072, Nov. 2015.

[2]R. De Doncker, D. Divan, and M. Kheraluwala, "A three phase soft switched high-power-density dc/dc converter for high-power applications," IEEE Trans. Ind. Appl., vol. 27, no. 1, pp. 63–73, Jan. 1991.

[3]J. Dudrik, P. Spanik, and N.-D. Trip, "Zero-voltage and zero-current switching full-bridge dc-dc converter with auxiliary transformer," IEEE Trans. Power Electron., vol. 21, no. 5, pp. 1328–1335, Sep. 2006.

[4]J.-G. Cho, C.-Y. Jeong, and F. Lee, "Zero-voltage and zero-current switching full-bridge PWM converter using secondary active clamp," IEEE Trans. Power Electron., vol. 13, no. 4, pp. 601–607, Jul. 1998.

[5]O. Patterson and D. Divan, "Pseudo-resonant full bridge dc/dc converter," IEEE Trans. Power Electron., vol. 6, no. 4, pp. 671–678, Oct. 1991.

[6]R. Steigerwald, "A comparison of half-bridge resonant converter topologies," IEEE Trans. Power Electron., vol. 3, no. 2, pp. 174–182, Apr. 1988.

[7]A. Bhat and R. Zheng, "Analysis and design of a three phase LCC-type resonant converter," IEEE Trans. Aerospace and Electron. Syst., vol. 34, no. 2, pp. 508–519, Apr. 1998.

[8] R. Steigerwald, "High-frequency resonant transistor dc-dc converters," IEEE Trans. Ind.

Electron., vol. IE-31, no. 2, pp. 181–191, May 1984

[9] X. Li, "A LLC-type dual-bridge resonant converter: Analysis, design, simulation, and experimental results," IEEE Trans. Power Electron., vol. 29, no. 8, pp. 4313–4321, Aug. 2014.

[10] J.-W. Kim and G.-W. Moon, "A new LLC series resonant converter with a narrow switching frequency variation and reduced conduction losses," IEEE Trans. Power Electron., vol. 29, no. 8, pp. 4278–4287, Aug. 2014.

[11] M. Deppenbrock, .Direct self control (DSC) of inverter-fed induction machine,. IEEE Trans. Power Electron., Vol. 3, pp. 420.429, July 1998.

[12] Bose.B.K., Modern Power Electronics and AC Drives, Prentice Hall, 2002

[13] Finch.J.W and Giaouris.D, . Controlled AC Drives., IEEE Trans. Ind. Electronics., Vol.55, No. 2, pp. 481.491, February 2008.

[14] Giuseppe Buja, Domenico Casadei and Giovanni Scrra, .Direct Torque Control of Induction Motor Drives., IEEE Catalog No.:97TH8280, ISIE.97-Guimaraes, Portugal, pp. TU2- TU8, 1997.

[15] D.Casadei, G.Serra, A.Tani and L.Zarri, .Assessment of Direct Torque Control for Induction Motor Drives., Bulletin of the Polish Academy of Sciences technical sciences, Vol. 54, No. 3, pp. 237-253, 2006.